Long-Term Tests of a DC Gas Insulated Transmission Line (DC GIL) embedded in Temporally Flowable Backfill: Soil-Mechanical and Thermic Interaction

Langzeitversuche an einer in zeitweise fließfähigen Verfüllbaustoff gebetteten DC Gasisolierten Leitung (DC GIL): Bodenmechanische und thermische Wechselwirkungen

Prof. Dr.-Ing. Thomas Neidhart, OTH Regensburg, thomas.neidhart@oth-regensburg.de
M.Eng. Maximilian Lerch, OTH Regensburg, maximilian.lerch@oth-regensburg.de
M.Eng. Doris Wiesinger, OTH Regensburg, doris.wiesinger@oth-regensburg.de
Dipl.-Ing. Martin Hallas, TU Darmstadt, hallas@hst.tu-darmstadt.de
Prof. Dr.-Ing. Volker Hinrichsen, TU Darmstadt, hinrichsen@hst.tu-darmstadt.de
Dr.-Ing. Michael Tenzer, Siemens Energy, Erlangen, michael.tenzer@siemens.com

Abstract

At present DC transmission systems for long distance transmission are of special interest, particularly with regard to transmission systems that proved ability for directly buried installation. Some service experience has been collected with directly buried AC GIL technology, but none with directly buried DC GIL. First pilot projects with directly buried AC GIL were designed conservative regarding the mechanical GIL support and the maximum allowable current. The aim is to optimize the mechanical and thermal design of directly buried DC GIL to offer cost efficient transmission line solutions.

Therefore, a ±550 kV DC GIL prototype with a current carrying capacity of 5000 A is currently investigated in a HVDC test facility, both in above-ground installation and a buried installation. This report presents results gained on the embedded installation for studying the soil mechanics and long-term thermic interaction with the backfill material and the adjacent soil. A DC GIL with a total length of 130 m is embedded in a temporarily flowable backfill ("TFB") as re-use of the excavated soil on site, which minimizes transportation costs and energy use. TFB is characterized by high contact forces that restrain the DC GIL displacements and by stable thermal conductivity, which optimizes the heat transfer. In order to monitor the mechanical soil-structure-interaction ("SSI"), various temperatures and moisture content sensors were installed inside and around the DC GIL, in the TFB and the adjacent soil as well down to 4 m below the ground surface. Displacement and strain sensors measured the elongations and dilatations of the embedded enclosure tube. Compressive stresses caused by restrained displacements are monitored with load cells. A fiber optical cable is used to monitor the temperatures in the aluminum conductor, on top and at the base of the enclosure tube, as well as in the TFB and the sand cover layer and the adjacent soil. The measurements were completed with some single sensors for temperature, moisture content and porewater-tensions which were mainly concentrated nearby the DC GIL in the TFB and the cover layer.

During 15 months, several load cycles impact on the embedded DC GIL. Each load cycle consists of a DC current feed of 5000 A for 4 weeks followed by another 4 weeks without current. Since the SSI is independent of voltage stress, this test is carried out with current only. After 4 load cycles only moderate temperatures are monitored at the enclosure tube and in the TFB, much lower as expected. Seasonal effects predominate the temperatures of the TFB, the cover layer and the adjacent soil, while the DC GIL generates only marginal increases. Moisture contents and porewater-tensions remain constant apart from some variations caused by rainfalls and vegetation cover. The elongation of the enclosure tube is shorter than 5 mm and the forces are lower than 500 kN. It can be concluded that the DC GIL with a current carrying capacity of 5000 A DC embedded in TFB shows temperature-rises far below the technical GIL limits after 4 load cycles. The TFB ensures high and stable heat conductivity and contact forces, thus restraining the GIL movement. The temperature-rises of the natural soil due to GIL heating are comparatively low in comparison to other effects like sun radiation. The TFB shows a good thermal and mechanical performance.

1 Introduction

In 2010 the first 1 km directly buried AC GIL with temporarily flowable backfill (TFB) was installed in the area of Frankfurt airport ("Kelsterbach") [1], [2]. This pilot installation was designed in a conservative way regarding the thermal and mechanical properties of the backfill. E.g. the current rating could be increased from 2700 A AC to 3150 A AC, since measured temperatures during operation remained far below the technical limits [3].

DC GIL solutions would be more competitive to other systems by utilizing the benefits of higher current ratings

and/or lower heating. Detailed thermal and mechanical measurements are thus required to further optimize the GIL rating calculations as well as the mechanical dimensioning of future directly buried GIL installations.

The directly buried DC GIL closes this gap and collects more data about mechanical soil-structure-interaction ("SSI"; e.g. displacements, strains, stresses, forces) and resulting temperatures when a DC current of 5000 A DC is fed into the directly buried DC GIL ("HL":= high load). Since the mechanical SSI is independent of high voltage stress, the test is carried out with current only. The gas compartments are filled with nitrogen with a total pressure p= 0,7 MPa and Δp = 0,6 MPa to the atmospheric pressure respectively. This represents a more critical thermal arrangement as with the N_2/SF_6 mixture, but allows easier gas handling. Differences of the measured temperature distribution when changing the gas parameters can easily be simulated.

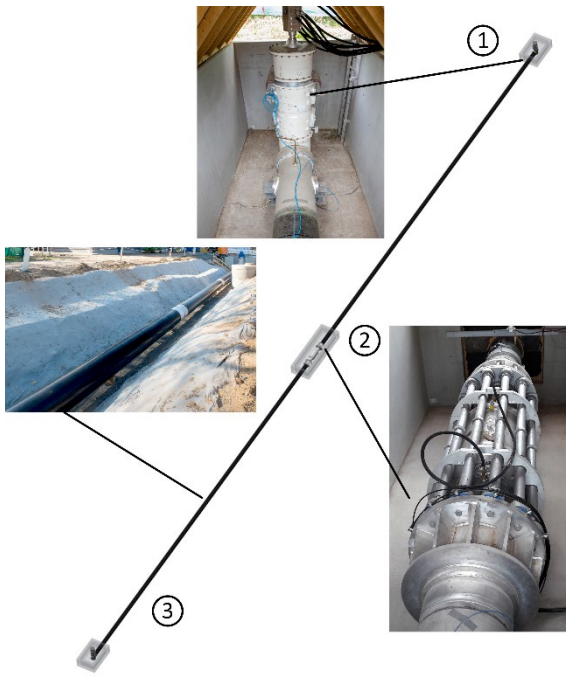

Figure 1 Soil mechanic test arrangement [10].

2 Test arrangement and tests

The directly buried DC GIL with a length of about 130 m is installed in a trench as shown in **Figure 1**. There are two concrete shafts at both ends of the GIL (1 and 3) and one in the center (2). At both ends (1 and 3) the GIL consists of an elbow module and a short vertical compartment, which is connected to the busbar of the power source. The busbar connection, as well as the steel structure is designed to allow a free movement of the GIL in axial direction, which is essential for the displacement measurement.

The center shaft (2) is used for mechanical measurements: The contact forces from "SSI" restraining the movement of the GIL enclosure tube in an area around the center of the installation result in compressive stresses in the enclosure tube, which can lead to buckling of the GIL enclosure. Load cells are installed to measure the axial forces inside the GIL enclosure tube by redirecting the axial forces. An axial compensator is used to make the enclosure tube flexible enough to not transfer axial forces. Brackets are welded to the enclosure tube on each side of the compensator. Steel beams in series with load cells connect the brackets (2) to measure the forces inside the enclosure tube.

The trench was excavated to a depth of 2.0 m (**Figure 2)** with 45° slope angles according to DIN 4124. The space between TFB (green area in Figure 2) and ground surface (height 0.75 m) is covered with the excavated soil, which allows simple agricultural use at practical installations. The conductor axis of the DC GIL runs horizontal 1.35 m below ground surface.

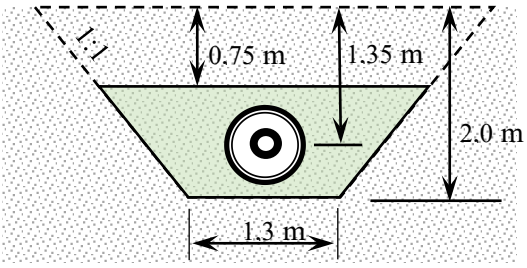

Figure 2 Cross section with trench geometry. Lower part of the trench filled with TFB (green area).

The embedded DC GIL is periodically stressed with high load ("HL") and current pauses to trigger GIL-soil displacements and to investigate the temperature rise. The first mechanical load cycles were 30 days "HL" cycle and 30 days zero load (0 A) so far (60 days in total). After four mechanical load cycles a current of 5000 A DC is constantly applied for 3 months starting end of May 2020. The results presented in the following were gained from June 1st 2019 until June 15th 2020 including four mechanical load cycles and another three weeks with a current of 5000 A DC.

3 Temporarily flowable backfill

The directly buried DC GIL is embedded in a temporarily flowable backfill (TFB). Major advantages of this material are re-use of the excavated material, high contact forces that restrains the GIL displacement and high and stable thermal conductivity to optimize heat transfer. Filling the trench with self-compacting TFB causes no vibrations, no dust and less noise than conventional sand backfill [7].

The soil mixture is adapted and optimized to the excavated sand before the construction work on site started using a sand sample of approximately 250 kg. The laboratory tests were made according to H-ZFSV [5] and result in a recipe of about 70 % excavated soil, 25 % water and 5 % bentonite and cement (mass percentage). This recipe provides after 15 min of mixing a stable suspension with pumpable and self-compacting capabilities.

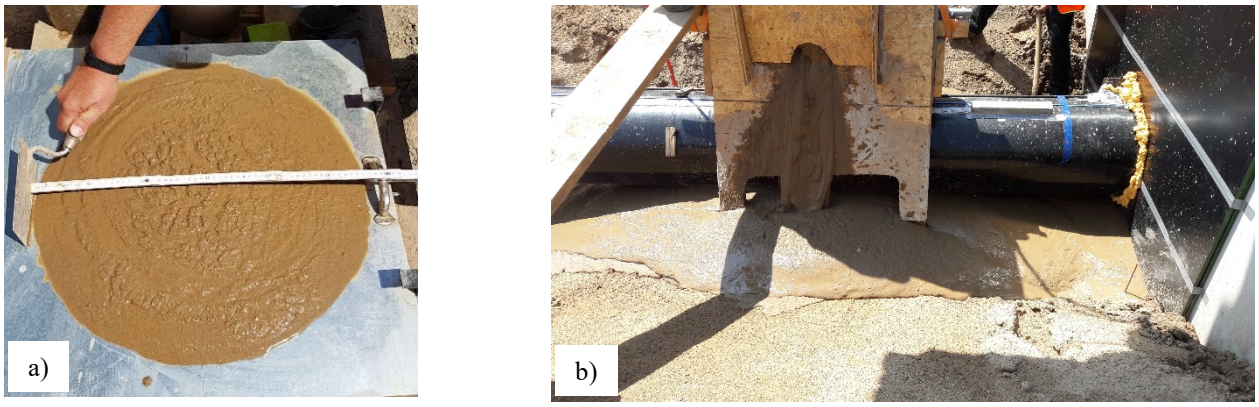

Figure 3 TFB on site. a) Slump/ consistency test. b) Pouring the stable TFB-suspension into the trench.

The TFB-qualities were checked by e.g. slump tests **(Figure 3 a)** for every charge before pouring the TPB into the trench. Bouyancy forces of the DC GIL were simply controlled by implementing a thin-layer back-step procedure **(Figure 3 b)** on site without buoyancy fixture. Lately after two hours, the suspension changed to solid state without bouyancy and could be covered with the next thin-layer of TFB. Meanwhile, the adjacent trench areas were refilled.

Further some other suitability tests were performed as uniaxial compressive strength of the hardened TFB which should remain lower than 0.35 MPa which correlates with a light re-excavation capability e.g. for maintenance purposes [5]. The adhesion and friction forces restrain the movement of the enclosure tube due to thermal expansion were determined by rod-shear-tests with lab scaled HDPE-rods. Based on these results, the restrained expansion of the GIL was predicted with a FE-Code in order to dimension the mechanical measurement equipment as load cells and extensometers (see Chapter 6).

The excavated natural sand on site shows ≈ 1.4 W/(m·K) tested with thermal conductivity ≈ 10 % water-content and ≈ 100 % Proctor-Density. The thermal conductivity of the sand decreases < 0.5 W/(m·K) at water-contents < 2 %. Further tests on TFB-samples prove a stable thermal conductivity in the range of 1.8 W/(m·K) neither without any significant reduction of the water content nor drying out for the expectable temperature of the embedding.

4 Soil temperature distribution

Figure 4 gives a review of the development of soil and air temperature and the rainfalls on site in the period from 1st June 2019 to 15th June 2020. The natural soil temperature was monitored at depth of 1.35 m below ground surface at the same depth as the conductor (see also Figure 2) but with a lateral distance of >10 m to the GIL axis. Air temperatures are depicted in Figure 4 as moving average of ±3 h and rainfalls are averaged over 15 min as usually. Weather data are monitored with a meteorological station placed on the test area. As expected, the soil temperature follows the oscillations of the air temperature in a damped way with a time lag and reaches max. 21°C in August 2019 and min. 4°C in February 2020.

The DC GIL was embedded in TFB in June 2019 at soil temperatures between 15 °C and 20 °C. The load cycles of heating (4 weeks with 5000 A DC) and zero load (4 weeks with 0 A) start at 16th September after a short current load test at 11th September. After 4 weeks of heating the conductor reaches a maximum temperature of approx. 68 °C

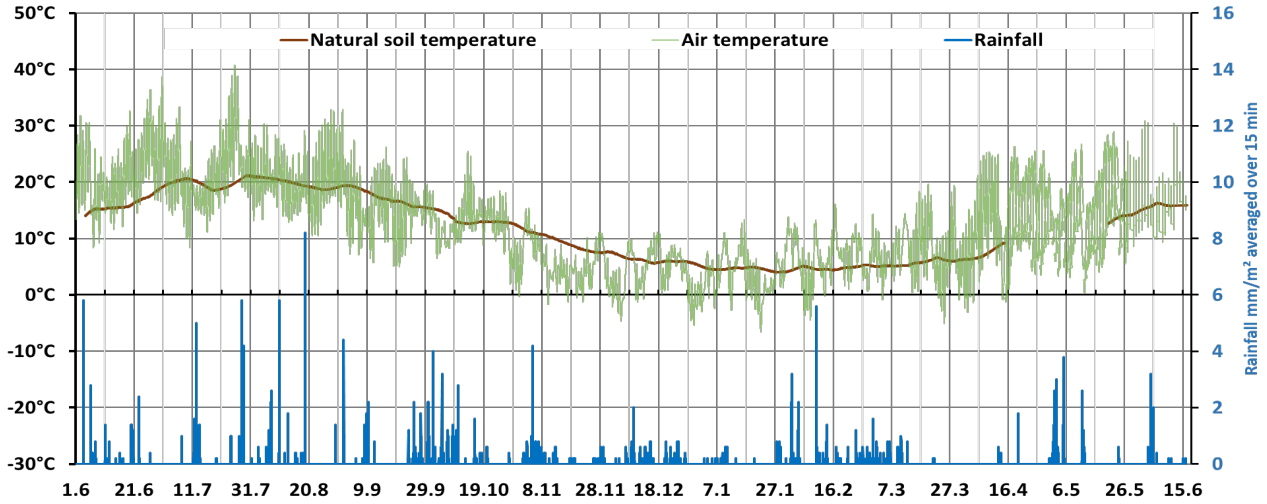

Figure 4 Temperature development and rainfalls on site (1.06.2019 – 15.06.2020)

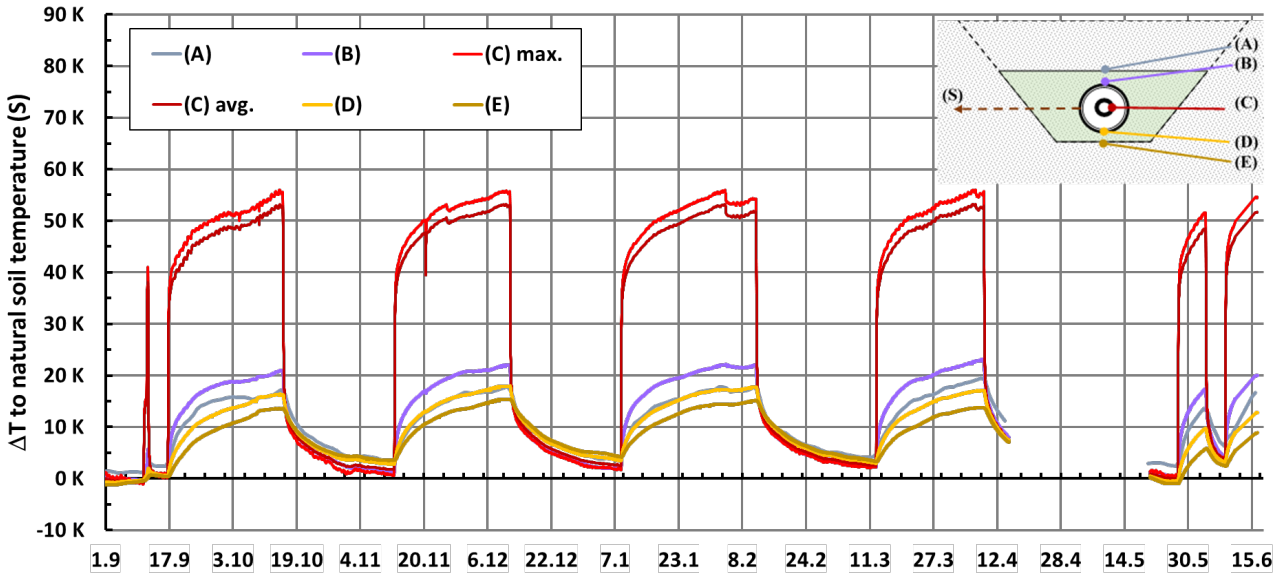

Figure 5 Development of the temperature differences ΔT (1.09.2019 – 15.06.2020) as difference of temperatures in the TFB (A, B, D, E) and natural soil temperature (S) with a lateral distance of 15 m to the GIL axis -1.35 m. For comparison temperature development of the conductor (C).

in the first load cycle. The temperatures at the housing and the TFB close to the GIL are lower than 35 °C.

In order to eliminate the decreasing air and soil temperatures over the seasons, which significantly affected the temperatures of the TFB and the GIL, in **Figure 5** the temperatures ΔT are depicted as difference to the natural soil temperature (S). The temperature differences ΔT between the conductor (C) and the natural soil (S) do still slightly increase after 4 weeks of heating, are repeatable in all cycles and remain < 60 K. The measured temperatures at the housing of the GIL are obviously lower than the temperature of the conductor and reach only ΔT = 23 K on top of the housing (B). Approximately 25 cm below the housing (E) at the contact surface between TFB and natural soil max. ΔT = 15 K is monitored. During cooling period the temperatures of the conductor are slightly lower than the temperatures of the housing due to the air contact of the GIL in the shafts (**Figure 5**). This also generates the oscillations of the conductor temperature, which are induced by the differences of the air temperatures on day and on night. The drop of temperature at 20th and the step at 26th November 2019 are caused by a short loss of power. An interruption of current source for one week happened in June 2020 which lead to a relevant drop of temperature. During the cooling of the 4th load cycle 4 from 15th May to 18th June 20 some problems appeared at the temperature monitoring system. Necessary repair implicated an extension of the cooling period from 4 to 7 weeks. This data gap also appears in Figure 4 at the natural soil temperature.

As completion to Figure 5, maximum temperature rises at each cross-section point for the first "HL" cycle from September to October 2019 are given in **Figure 6** at the housing to a lateral distance of 16 m. The temperature rises are defined as the differences of temperatures before and after four weeks of "HL" current stress. The average ambient temperature before the test was in the range of 20 °C. The temperature rise of the GIL conductor is reproducible in both cycles and remains < 60 K. The measured temperature rise at the enclosure tube reaches a maximum of ΔT = 21 K on its top. The maximum temperature gradient at the insulators is thereby 30 K. The ambient temperature decreased during the first "HL" cycle because of changes in the weather. The temperature rise of the sensors with 3 m, 4 m and 16 m distance is therefore negative.

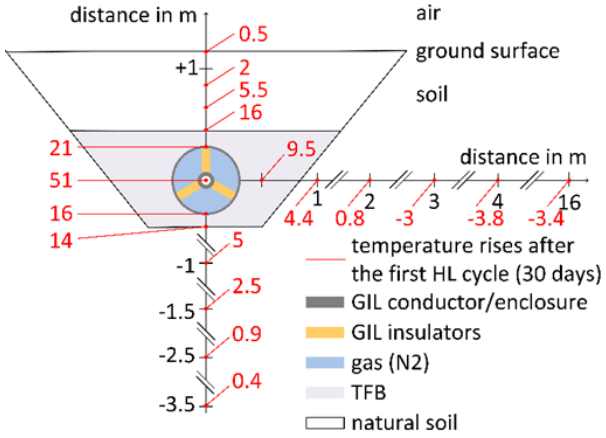

Figure 6 TFB-embedded GIL cross section: Monitored maximum temperature rises after the first HL cycle

The measured maximum temperatures for all heating cycles are nearly the same. In the case of a drop of thermal conductivity, the measured maximum temperatures in sand or TFB would decrease for the following heating periods.

These results are generally confirming the comparatively low increase of temperature for GIL, even in this worst case scenario test with permanent 5000 A DC energization and with thermally unfavorable 100 % N_2 gas insulation of the DC GIL specimen. Due to the currents' square influence on the temperature increase, a significantly lower thermal condition in service with lower current ratings and/or partial load of the DC GIL transmission system is therefore to be expected.

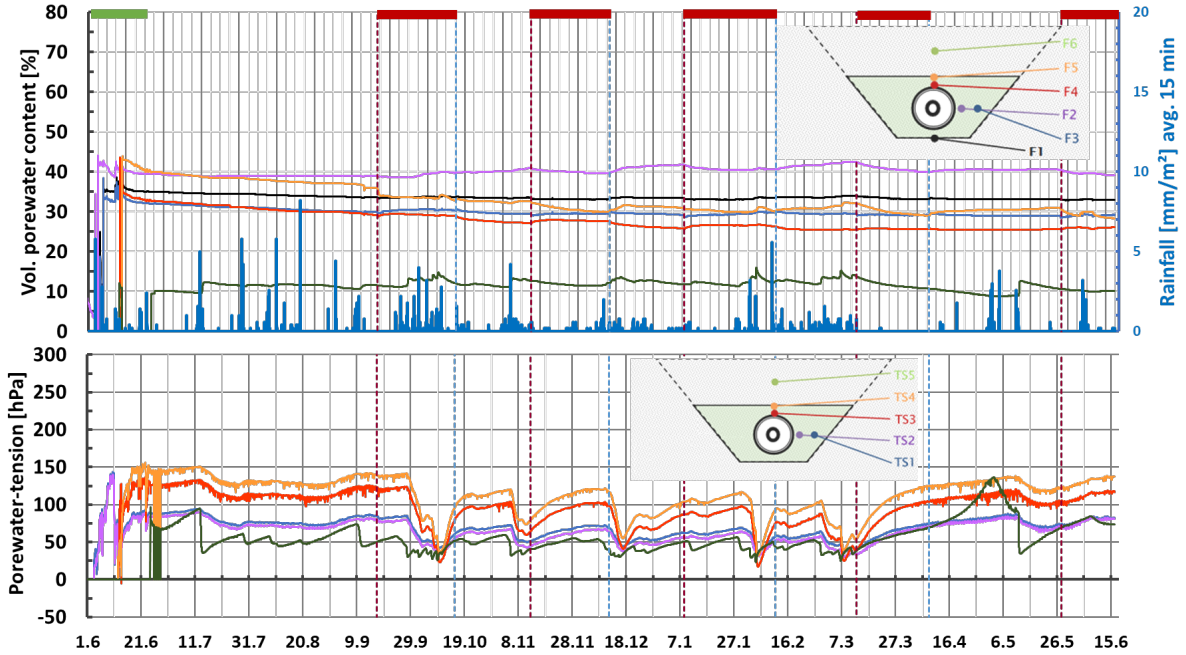

Figure 7 Development of volumetric porewater content (F1 –F6), porewater tensions (TS1 – TS5) and rainfall averaged over 15 minutes (1.06.2019 – 15.06. 2020).

5 Water contents and potential

Porewater content has a huge influence on the thermal conductivity of soil. Usually an increase of water content leads to an increase of thermal conductivity. The energy state of water in porous media like soil and therefore movement of water is reflected by porewater potential. So, there's a relationship between water content, porewater water potential, thermal conductivity and temperature distribution [9].Therefore, the developments of the volumetric porewater content and the porewater potential were measured **(Figure 7)**. The volumetric porewater content was monitored with TDR soil moisture sensors (Figure 7 upper part) and the porewater potential with tensiometers (Figure 7 lower part). Figure 7 is completed with the measured rainfall average over a period of 15 minutes as usual.

A tensiometer consists of a water filled acrylic glass shaft, a ceramic tip and pressure sensor. The water in the tensiometer is in contact with the porewater. A tension (positive sign) is sensed, if the matrix potential of the surrounding soil is lower than the pressure in the tensiometer. Drying out of the soil leads to increasing porewater-tensions. Otherwise, porewater-pressure (negative sign) indicates a tensiometer e.g. below the groundwater table. An increase of porewater-tensions and decrease of porewater-contents during heating cycle would have been expected for different reasons. The heat may induce complete drying-out of the bedding area close to DC GIL as described in [7] for sand. The development of the measured date **Figure 7** show that porewater-tensions and porewater contents are not significantly affected by heating. In the monitoring period 1.06.2019 to 15.06.2020, porewater contents and tensions in the TFB are approximately constant in a range of 25 to 45% and < 150 hPa. Only dry periods or rainfalls cause significant changes of the porewater tensions. Remarkable decrease of porewater tensions correlate with rainfalls which is obvious at the end of the heating periods with the highest temperature, e.g. Oktober 2019 and February 2020.

Only TDR-sensor F6 and the tensiometer TS5 (green curves) show rather specific developments of volumetric porewater content and porewater tensions because these sensors were placed in the sand cover layer and not in TFB. The volumetric porewater content (F6) remained < 16 % and was very sensitive to rainfall and dry periods. Porewater tensions (TS5) in the sand cover layer strongly increase in April 2020 while the TFB porewater tensions are slightly affected. Consequently, porewater content of the adjacent natural soil (sand) would strongly decrease in periods without any rainfall incidents. A long-lasting dry period may result in a completely drying out of the adjacent sand. TFB provides much stable hydraulic and thermal soil properties in contrast to the natural soil (sand) on site and on top.

6 Soil-structure-interaction

Another essential aspect of the buried DC GIL is to monitor the strains and the displacements of the GIL-housing in order to verify the results of laboratory tests and to calibrate the FE-calculations for further design. With regard to the importance to monitor the displacements during the load cycles some theoretical mechanical aspects of the SSI of a TFB-embedded GIL shall be discussed first [6]. Therefore, the mechanical SSI assembly, which is depicted in a longitudinal section in **Figure 8,** can be simplified to an equivalent static system of a cantilever with a fixed-end (x =0) at shaft 2 (Figure 1) but embedded from x = 0 to 1.0 in shaft 1 (Figure 1). The small gap at shaft 2 between x = 0 and the fixed-end can be neglected. Heating of the cantilever

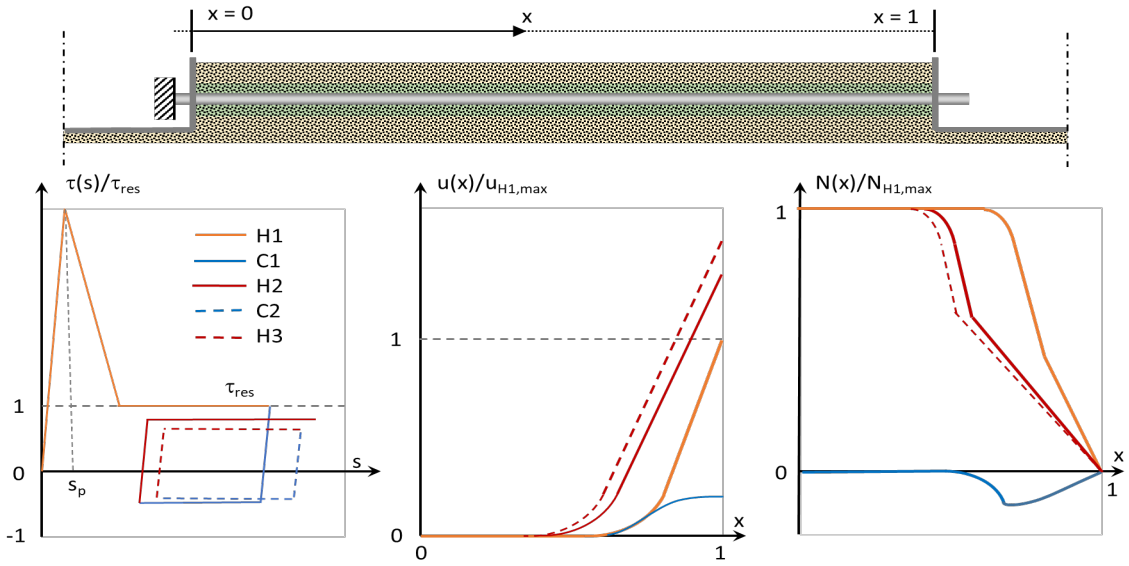

Figure 8 Axial SSI of TFB-embedded GIL-housing. Top: Equivalent static system. Left: Simplified and normalized shear resistance τ(s) at the interface TFB/HDPE-coating. Middle: Normalized axial displacements u(x). Right: Normalized axial force N(x).

will cause expansion, which leads to displacements u(x) with u_{max} at the unrestrained end x = 1 in shaft 1.

The graph on the left side in Figure 8 represents the simplified axial shear resistance τ(s) of TFB as a function of displacement s. It should be pointed out that τ(s) depends on several other parameters like TFB-recipe, contact material, overburden pressure, curing time, etc. For the first heating H_1 and $s < s_p$ the constitutive behavior of τ(s) is more or less elastic. The peak resistance of adhesion is reached at $s = s_p$, followed by a hyperbolic softening of τ(s) to a residual shear resistance τ_{res} for $s >> s_p$, here simplified with two linear lines. The constitutive behavior of residual shear resistance τ_{res} can be approximated as sliding friction. The first cooling C_1 generates negative shear resistance which becomes again positive with the second heating H_2. It is noteworthy, that no adhesive peak occurs at H_2 and the following heating. As long as the temperature of the housing remains lower or equal the temperature in H_1, the shear resistance does not reach the level τ_{res} again but shows a shakedown. After 4 cycles a least, τ(s) adjusts to the dashed lines (H_n, C_n) in Figure 8. This behavior of τ(s) results in load cycle dependent axial displacements u(x) and axial force N(x) distributions which are illustrated in the middle and the right graph of Figure 8. Even in case as depicted in Figure 8 with the same and constant level of housing temperatures during heating and cooling ($T_{H1} = T_{H2} = \ldots T_{Hn}$ and $T_{C1} = T_{C2} = \ldots T_{Cn}$ for 1 to n cycles), it is complex to calculate u(x) and N(x). An important effect is that the displacements u(x) increase cycle per cycle until the shear resistance adjusts (dashed lines). Max. axial force $N_{H1,\,max}$ does not change as long as $T_{H1} = T_{H2} = \ldots T_{Hn}$ and can be

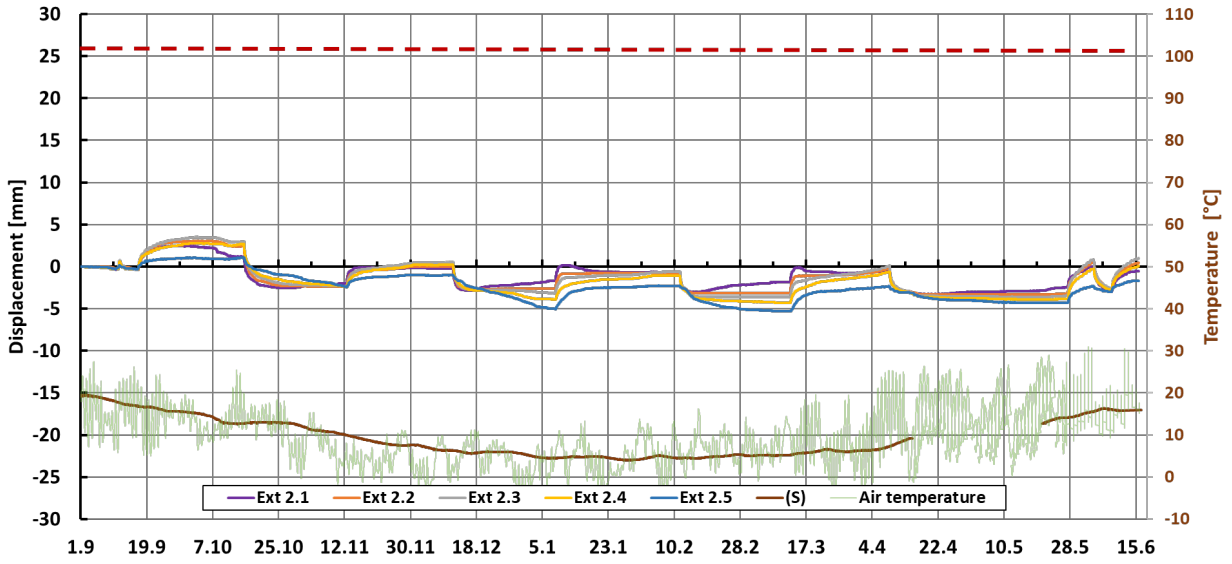

Figure 9 Measured displacements of the GIL-housing (Ext 2.1 – Ext 2.5), natural soil temperature (S) – 1.35 m and air temperature from 1.09.2019 – 15.06.2020.

calculated by $N_{H1,\,max} = A_O \cdot E \cdot \alpha \cdot \Delta T$ for a tube with two fixed-ends and completely restrained displacements, with cross-section area of the housing A_O, coefficient of elasticity E, thermal expansion coefficient α and temperature difference ΔT. Positive axial forces (compression) occur during heating, negative axial forces (tension) during cooling.

Mechanical extensometers (DIN EN ISO 18674-2) are placed on top of the housing with approximately equally spaced fixed tips over the complete length of the TFB-embedded housing. The displacements of the fixed tips are measured with electronic displacements sensors with a resolution of ± 0.1 mm. The chosen arrangement of the extensometers makes it possible to monitor the axial displacements of the GIL-housing between the fixed tips and shaft 2. Additional extensometer type sensors are installed to monitor the radial expansions and compression of the TFB-embedded GIL-housing.

The measured displacements of the GIL-housing between shaft 2 and 3 are in a range of +/- 5 mm from 1st September 2019 to 15th June 2020 after four heating cycles (**Figure 9).** Each heating cycle caused displacements $u_{max} < 5$ mm superposed with the displacements caused by seasonal soil temperature change represented by the natural soil temperature (S). It is not of importance to discuss each extensometer displacement because the values are small. For comparison, the displacement of a completely free and not embedded aluminum bar, which generates $u \approx 26$ mm for $\Delta T = 20$ K, is marked with a red dashed line in Figure 8. With respect of the monitored displacements, it can be concluded that the mobilized shear resistance is lower than peak resistance of adhesion. TFB and GIL-housing have an "elastic" contact behavior.

The measured axial forces correlate to the measured temperature differences ΔT at the housing and remain in the predicted ranges lower than 500 kN. Both, the axial forces and the displacements well accord with the results of the calculations. More graphs of the displacements and axial forces will be published and discussed after finishing the field test.

7 Conclusions

The soil-structure interaction as well as the temperature rise are investigated at a directly buried 130 m long DC GIL. It is embedded in temporarily flowable backfill, which ensures high and stable heat conductivity and high contact forces that restrain the GIL movement. The moisture content of the backfill is proven to remain constantly stable, even during longer dry periods, which thereby ensures its mechanical and thermal properties. The test is performed at DC current only, without voltage applied. Four high load cycles show temperatures far below the technical limits of the GIL. The temperature rise of the natural soil due to GIL heating is comparably lower to other effects like sun radiation. It is assumed that the heated GIL would not influence the natural growth. The temporary flowable backfill effectively reduces the expansion and displacements of the GIL-housing. So far, approximately elastic deformation at the soil-structure interaction was observed. The displacements of the GIL were below 5 mm. The results clearly show, that feared gaps between backfill and enclosure tube as well as neither lifting or buckling of the enclosure tube due to thermal forces will not occur in practice. Further HL to evaluate the technical limits of the systems will be carried out during the next months.

8 Acknowledgments

The authors gratefully acknowledge the substantial support of this work by the German Federal Ministry of Economics and Technology (Funding Code 03ET7546).

Supported by:
Federal Ministry for Economic Affairs and Energy
on the basis of a decision by the German Bundestag

9 Literature

[1] Koch, H.: Gas-Insulated Transmission Lines, ISBN 978-0-470-66533-6, IEEE Press / John Wiley & Sons, 2012.

[2] Neumann, C.; Poehler, S.: First Pilot Installation of a 380 kV directly buried Gas Insulated Line (GIL), In: Jicable Conference, Versailles – France, Paper B5.6., 19 - 23 June 2011

[3] Poehler, S.; Rudenko, P.: Directly buried gas-insulated transmission lines (GIL), In: PES T&D, USA, Orlando, FL, pp. 1-5, 7-10 May 2012

[4] Magier, T.; Tenzer, M.; Koch, H.: "Direct Current Gas-Insulated Transmission Lines", IEEE Transactions on Power Delivery, Vol. 33, No. 1, Pp. 440-446, ISSN 0885-8977, February 2018.

[5] H ZFSV – Hinweise für die Herstellung und Verwendung von zeitweise fließfähigen, selbstverdichtenden Verfüllbaustoffen. FGSV - Forschungsgesellschaft für Straßen- und Verkehrswesen e.V., Köln, 2012.

[6] Wagner, B.: Ein Beitrag zur axialen Bettung von Kunststoffmantelrohren der Fernwärme in ZFSV, Schriftenreihe der TU Bergakademie Freiberg, Institut für Bergbau und Spezialtiefbau, Professur für Erdbau und Spezialtiefbau, Heft 9, 2018.

[7] Neidhart, T.: Bodenmechanische und erdbautechnische Aspekte der Erdverkabelung, in Beiträge zum 17. Geotechnik-Tag in München, Heft 64: Zusammenwirken von Forschung und Praxis der Schriftenreihe, Lehrstuhl und Prüfamt für Grundbau, Bodenmechanik, Felsmechanik und Tunnelbau, Cudmani, R. (Hrsg.).

[8] CIGRE 714: Longterm performance of soil and backfill systems. CIGRE WG B1.41, December 2017.

[9] Durner, W.; Flühler, H.: Soil Hydraulic Properties. In: Encyclopedia of Hydrological Sciences, S. 1103–1119, 2005

[10] M. Hallas, V. Hinrichsen, C. Neumann, M. Tenzer, B. Hausmann, D. Gross, T. Neidhart, M. Lerch, D. Wiesinger: Cigré Prototype Installation Test for Gas-Insulated DC Systems – Testing a Gas-Insulated DC Transmission Line (DC-GIL) for ±550 kV and 5000 A under Real Service Conditions. CIGRE D1-107, 2020.